

## Supporting Information

### **Transformable nanotherapeutics enabled by ICG: Towards enhanced tumor penetration under NIR light irradiation**

Yuxiang Tang<sup>a,b,#</sup>, Yihui Li<sup>a,b,#</sup>, Si Li<sup>a,b,#</sup>, Hang Hu<sup>a,b</sup>, Yuxin Wu<sup>a,b</sup>, Chen Xiao<sup>a,b</sup>, Zhiqin Chu<sup>c</sup>,  
Zifu Li<sup>a,b,d,e,\*</sup>, and Xiangliang Yang<sup>a,b,d</sup>

<sup>a</sup>Department of Nanomedicine and Biopharmaceuticals, College of Life Science and Technology, Huazhong University of Science and Technology, Wuhan, 430074, China

<sup>b</sup>National Engineering Research Center for Nanomedicine, College of Life Science and Technology, Huazhong University of Science and Technology, Wuhan, 430074, China

<sup>c</sup>Department of Electrical and Electronic Engineering, Joint appointment with School of Biomedical Sciences, The University of Hong Kong, Hong Kong

<sup>d</sup>Hubei Key Laboratory of Bioinorganic Chemistry and Materia Medica, Huazhong University of Science and Technology, Wuhan, 430074, China

<sup>e</sup>Wuhan Institute of Biotechnology, High Tech Road 666, East Lake high tech Zone, Wuhan, 430040, China

Author Contributions: #These three authors contributed equally to this work.

\*Corresponding author:

Professor Zifu Li

Tel.: 86 27 87792234, Fax: 86 27 87792234, E-mail: [zifuli@hust.edu.cn](mailto:zifuli@hust.edu.cn)

## Experiment section

### Materials

HES 40/0.5 with average molecular weight (Mw) 40 kDa and hydroxyethyl substitution degree of 50% was a gift from Wuhan HUST life Sci & Tech Co., Ltd. (Wuhan, China). 3,3'-dithiodipropionic acid (DTDPA, 99%), octanedioic acid (ODA, 99%), dicyclohexyl carbodiimide (DCC, 99%), 4-dimethylaminopyridine (DMAP, 99%), (N-ethyl-N'-(2-(dimethylamino) propyl) carbodiimide hydrochloride (EDCI, 98%), and N-hydroxysuccinimide (NHS,98%) were purchased from J&K Chemical Reagent Inc. (Shanghai, China). Salmon fibrinogen and thrombin were purchased from Pfenex Inc (San Diego, CA, USA). All other chemicals were of analytical grade and used as received, except for dimethyl sulfoxide (DMSO), which was dried with 4 Å molecular sieves before use.

### Synthesis and Characterization of HES-SS-DOX

#### Synthesis

HES-SS-DOX was synthesized according to a procedure described elsewhere<sup>1</sup>. The amount of DOX conjugated to the drug conjugates was determined by UV/vis spectrophotometry at 480 nm using a standard calibration curve. Drug loading (DL) of the conjugates was calculated according to the following formula:

$$DL (\%) = \frac{Wt (drug)}{Wt (conjugates)} \times 100\% \quad (1)$$

Where Wt (drug) is the weight of drug in the drug conjugates, and Wt (drug conjugates) is the weight of the conjugates. The DL of DOX in the synthesized HES-SS-DOX calculated by Eq. (1) is 5.5 wt%, corresponding to around 5 DOX molecules per HES.

#### Characterization

<sup>1</sup>H-NMR spectra were recorded on a nuclear magnetic resonance spectrometer (Ascend™ 600 MHz, Bruker) using tetramethylsilane (TMS) as an internal reference. FT-IR spectra were recorded on a fourier transform infrared spectrometer (Vertex70, Bruker) with an attenuate total reflection accessory. UV/vis spectra were recorded on a UV/vis spectrophotometer (TU-1901, Beijing Purkinje General Instrument Co., Ltd.). Fluorescence spectra were recorded on a fluorescence spectrophotometer (F-4500, Hitachi). The

hydrodynamic diameter was measured by dynamic light scattering (DLS, Nano-Zs90, Malvern) at the concentration of 2 mg/mL. The morphology of ICG@HES-SS-DOX NP was characterized by transmission electron microscopy (TEM, Tecnai G2, FEI, Holland) operated at an accelerating voltage of 100 KV.

#### **Preparation of HES-SS-DOX NP**

HES-SS-DOX NP was fabricated by a Pickering emulsion/solvent evaporation method<sup>2</sup>. Briefly, 10 mg of HES-SS-DOX was suspended in 10 mL of deionized water. To the suspension, 100  $\mu$ L oil solution (mixed methanol/chloroform solution) was added and the resulting mixture was sonicated for 5 min (Scientz-IIID, Ningbo Scientz Biotechnology Co., Ltd). Then the methanol/chloroform inside the formed Pickering emulsion was removed by vacuum evaporation and the resulting suspension was lyophilized for further use.

#### **Preparation of ICG@HES-SS-DOX NP**

ICG-loaded HES-SS-DOX NPs were prepared by a Pickering emulsion/solvent evaporation method<sup>2</sup>. Briefly, 10 mg of HES-SS-DOX was suspended in 10 mL of deionized water. To the suspension, 100  $\mu$ L of ICG oil solution (certain amount of ICG was dissolved in methanol/chloroform mixed solution) was added and the resulting mixture was sonicated for 5 min (Scientz-IIID, Ningbo Scientz Biotechnology Co., Ltd). The methanol/chloroform was removed by vacuum evaporation. Then the resulting suspension was dialyzed overnight to remove free ICG, and lyophilized for further use. The drug loading of DOX and ICG of the prepared nanoparticles was quantified by UV/Vis spectrophotometer.

#### **In vitro drug release study**

The release profile of DOX from HES-SS-DOX and ICG@HES-SS-DOX NP were studied using a dialysis method at 25 °C in four different media<sup>1</sup>, including PBS buffer (10 mM, pH 7.4, Tween-80 0.5%) without DTT, PBS buffer (10 mM, pH 7.4, Tween-80 0.5%) with 2  $\mu$ M DTT, PBS buffer (10 mM, pH 7.4, Tween-80 0.5%) with 2 mM DTT, and PBS buffer (10 mM, pH 7.4, Tween-80 0.5%) with 10 mM DTT. Briefly, 1 mL of HES-SS-DOX (10.0 mg) or ICG@HES-SS-DOX NP (11.4 mg) were placed in a dialysis tube (MWCO

3500 Da). The tubes were immersed in 40 mL of release media and shaken at a speed of 200 rpm at 25 °C. At desired intervals, 2.0 mL of release media was taken out and replenished with equal volume of fresh media. The amount of released DOX was determined by UV/Vis spectrophotometer (TU-1901, Beijing Purkinje General Instrument Co., Ltd.). The monitoring UV wavelength was 480 nm. The release experiments were conducted in triplicate. The presented results are the average values with standard deviations.

#### **The effect of NIR irradiation time on ICG@HES-SS-DOX NP dissociation**

1 mg of ICG@HES-SS-DOX (DOX loading rate of 4.8%, ICG loading rate of 12.5%) was suspended in 1.0 mL of deionized water. ICG@HES-SS-DOX solution was diluted 12.5 times (10 µg/mL of ICG). 7 mL of the suspension were taken out and then equally separated into 7 groups. The groups were stimulated by NIR laser at 25 °C (water bath) for 0, 0.5, 1, 2, 3, 4, 5 min, respectively (808 nm, 1.0 W/cm<sup>2</sup>). The morphologies of nanoparticles were characterized by TEM. The samples for TEM imaging were prepared by placing a small drop of the prepared ICG@HES-SS-DOX suspension onto a carbon-coated copper grid and dried at room temperature, followed by negatively staining with phosphotungstic acid at a concentration of 0.2% (w/w) for 1 min. The count rates were recorded by dynamic light scattering (DLS, Nano-ZS90, Malvern). The absorbance of each group was measured by UV/Vis. ICG emission spectra and DOX emission spectra of each group were monitored by fluorescence spectrophotometer at the excitation wavelength of 730 nm and 480 nm, respectively. The temperature was recorded at 30 s intervals using an infrared imaging camera.

#### **The effect of NIR light power on the dissociation of ICG@HES-SS-DOX NP**

1 mg of ICG@HES-SS-DOX (DOX loading rate of 4.8%, ICG loading rate of 12.5%) was suspended in 1.0 mL of deionized water. ICG@HES-SS-DOX solution was diluted 12.5 times (10 µg/mL of ICG). 7 mL of the suspension was taken out and then equally divided into 7 groups. The groups were stimulated by NIR laser for 0, 0.5, 1, 2, 3, 4, 5 min, respectively (808 nm, 2.0 W/cm<sup>2</sup>). The absorbance of each group was measured by UV/Vis.

#### **Interaction between ICG and ICG**

A certain amount of ICG was dissolved in deionized water to achieve different concentrations of ICG suspension (10, 25, 50, 75, 100, 200, 300 µg/mL) at 25 °C. Immediately, the absorbance of each sample was measured by UV/Vis spectrophotometer.

#### **The function of ICG in ICG@HES-SS-DOX NP**

A certain amount of HES-SS-DOX, HES-SS-DOX NP were dissolved in deionized water to achieve 5.8 µg/mL DOX at 25 °C. A certain amount of HES-SS-DOX mixed with ICG, a certain amount of HES-SS-DOX NP mixed with ICG and a certain amount of ICG@HES-SS-DOX NP were dissolved in deionized water to achieve 5.8 µg/mL DOX and 15 µg/mL ICG at 25 °C. A certain amount of ICG was dissolved in deionized water to achieve 15 µg/mL ICG. Then, the absorbance of each group was measured by UV/Vis spectrophotometer.

#### **Interaction between ICG and DOX**

1 mg of ICG was dissolved in 100 mL of deionized water to achieve 100 mL of ICG solution (ICG concentration 10 µg/mL). Then, certain amounts of DOX were dissolved in deionized water to achieve 0 µg/mL, 1 µg/mL, 4 µg/mL, 7 µg/mL, 10 µg/mL, 15 µg/mL and 20 µg/mL solution, respectively. Next, DOX solution with different concentrations was mixed with 10 µg/mL ICG solution at volume ratio of 1:1 (mL: mL). The absorbance of each mixed sample was measured by UV/Vis spectrophotometer. ICG emission spectra of each mixed sample was monitored by fluorescence spectrophotometer at the excitation wavelength of 730 nm.

#### **Interaction between ICG and HES-SS-DOX**

1 mg of ICG was dissolved in 100 mL of deionized water to achieve 100 mL of ICG solution (ICG concentration 10 µg/mL). Then, certain amounts of HES-SS-DOX were dissolved in deionized water to achieve solution with the DOX concentration of 0 µg/mL, 1 µg/mL, 4 µg/mL, 7 µg/mL, 10 µg/mL, 15 µg/mL and 20 µg/mL solution, respectively. Next, HES-SS-DOX solution with different concentrations was mixed with the 10 µg/mL ICG solution at volume ratio of 1:1 (mL: mL). The absorbance of each mixed sample was measured by UV/Vis spectrophotometer. ICG emission spectra of each mixed sample was monitored by fluorescence spectrophotometer at the excitation wavelength of 730 nm.

#### **Interaction between DOX and ICG**

1 mg of DOX was dissolved in 100 mL of deionized water to achieve 100 mL of DOX

solution (DOX concentration 10 µg/mL). Then, certain amounts of ICG solution were dissolved in deionized water to achieve 0 µg/mL, 1 µg/mL, 4 µg/mL, 7 µg/mL, 10 µg/mL, 15 µg/mL and 20 µg/mL solution, respectively. Next, ICG solution with different concentration was mixed with the 10 µg/mL DOX solution at volume ratio of 1:1 (mL: mL). The absorbance of each mixed sample was measured by UV/Vis spectrophotometer. DOX emission spectra of each mixed sample was monitored by fluorescence spectrophotometer at the excitation wavelength of 480 nm.

#### **Interaction between HES-SS-DOX and ICG**

18.2 mg of HES-SS-DOX was dissolved in 100 mL of deionized water to achieve 100 mL of DOX solution (DOX concentration 10 µg/mL). Then, certain amounts of ICG solution were dissolved in deionized water to achieve 0 µg/mL, 1 µg/mL, 4 µg/mL, 7 µg/mL, 10 µg/mL, 15 µg/mL and 20 µg/mL solution, respectively. Next, ICG solution with different concentrations was mixed with the 10 µg/mL DOX solution at volume ratio of 1:1 (mL: mL). The absorbance of each mixed sample was measured by UV/Vis spectrophotometer. DOX emission spectra of each mixed sample was monitored by fluorescence spectrophotometer at the excitation wavelength of 480 nm.

#### **Preparation of ICG@HES-SS-DOX NP with varied ICG loading content**

Certain amounts of ICG were dissolved in methanol/chloroform mixed solution to achieve 0 mg/mL, 0.5 mg/mL, 1 mg/mL, 1.5 mg/mL, 2.0 mg/mL, 2.5 mg/mL ICG solution, respectively. Next, 100 µL of the ICG oil solution with different concentrations was added into the 1 mL of HES-SS-DOX (DOX concentration 1mg/mL) solution and the resulting mixture was sonicated for 5 min using a probe-type ultrasonic device (Scientz- II D, Ningbo Scientz Biotechnology Co., Ltd). The methanol/chloroform inside the formed Pickering emulsion was removed by vacuum evaporation. The obtained supernatant was then dialyzed against deionized water for 1 day (MWCO: 3500 Da) to fully remove free ICG, and lyophilized for further use. The drug loading of ICG of the prepared nanoparticles was quantified by UV/Vis spectrophotometer. Briefly, a certain amount of freeze-dried ICG@HES-SS-DOX was dissolved in DMSO. The absorbance of ICG at 730 nm was used for determining the drug loading of ICG.

ICG@HES-SS-DOX with varied ICG loading rate was negatively stained by 0.2% (w/w)

phosphotungstic acid and then its morphology was measured by TEM. The diameter distribution of ICG@HES-SS-DOX NP was measured by DLS.

#### **Influence of ICG loading content on the ICG@HES-SS-DOX NP dissociation**

1 mL of ICG@HES-SS-DOX NP (DOX concentration 3.8  $\mu\text{g/mL}$ ) with different ICG loading content (0 wt%, 4 wt%, 7.5 wt%, 12.5 wt%, 17.1 wt%, 19.4 wt%) were stimulated with NIR laser (808 nm, 1.0  $\text{W/cm}^2$  or 2.0  $\text{W/cm}^2$ ) for 5 min. Then, ICG@HES-SS-DOX NPs with different ICG loading rate (0 wt%, 4 wt%, 7.5 wt%, 12.5 wt%, 17.1 wt%, 19.4 wt%) were negatively stained by 0.2% (w/w) phosphotungstic acid and then their morphologies were characterized by TEM. The size distribution of ICG@HES-SS-DOX NP with different ICG loading content (0 wt%, 4 wt%, 7.5 wt%, 12.5 wt%, 17.1 wt%, 19.4 wt%) were also measured by DLS.

#### **The degradation of ICG over time in deionized water/PBS buffer**

Degradation of ICG over time in deionized water/PBS buffer was monitored by UV/Vis. Briefly, certain amounts of ICG were solved in deionized water/PBS buffer to achieve 3 mL of ICG solution (10  $\mu\text{g/mL}$ ). Then, the UV absorbance of ICG in deionized water/PBS buffer was detected by UV/Vis spectrophotometer from day 1 to day 7.

#### **The degradation of ICG over time in serum solution**

Degradation of ICG in mice serum was monitored by UV/Vis. Briefly, certain amounts of ICG were solved in deionized water and mice serum mixtures at volume ratio of 9:1 (mL: mL) to achieve 3 mL of ICG solution (10  $\mu\text{g/mL}$ ). Then, the UV absorbance of ICG in serum solution was detected by UV/Vis spectrophotometer from day 1 to day 8.

#### **The dissociation of ICG@HES-SS-DOX NP over time**

The dissociation of ICG@HES-SS-DOX NP was monitored by UV/Vis, DLS and TEM over time. Briefly, certain amounts of ICG@HES-SS-DOX NP were dissolved in deionized water/PBS buffer to achieve 3 mL of ICG@HES-SS-DOX NP solution (ICG concentration 10  $\mu\text{g/mL}$ ). Then, the UV absorbance of ICG of ICG@HES-SS-DOX NP in deionized water/PBS buffer was detected by UV/Vis spectrophotometer from day 1 to day 7. The size distribution and count rate of ICG@HES-SS-DOX NP were monitored by DLS from day 1 to day 7, respectively. The morphology of ICG@HES-SS-DOX NP was measured by TEM at day 1, day 4 and day 7, respectively.

### **The dissociation of ICG@HES-SS-DOX NP in mice serum over time**

The dissociation of ICG@HES-SS-DOX NP in mice serum was monitored by UV/Vis over time. Certain amounts of ICG@HES-SS-DOX NP were dissolved in mice serum and deionized water mixtures at volume ratio of 1:9 (mL: mL) to achieve 3 mL solution (ICG concentration 10 µg/mL). Then, the UV absorbance of ICG@HES-SS-DOX NP in serum was detected by UV/Vis spectrophotometer from day 1 to day 8. The size distribution of ICG@HES-SS-DOX NP before and after 10 min NIR (808 nm, 1.0 W/cm<sup>2</sup>) stimulating at day 4, day 5 and day 8 were monitored by DLS, respectively.

### **The effect of temperature on the dissociation of ICG@HES-SS-DOX NP**

The effect of temperature on the dissociation of ICG@HES-SS-DOX NP was studied by UV/Vis, DLS and TEM. Briefly, 1 mg of ICG@HES-SS-DOX (DOX loading content of 4.8%. ICG loading content of 12.5%) was suspended in 1.0 mL deionized water. ICG@HES-SS-DOX solution was diluted 12.5 times (10 µg/mL of ICG). 7 mL of the suspension were taken out and then equally divided into 7 groups, each group was stimulated by NIR laser at 25 °C (water bath) for 0, 0.5, 1, 2, 3, 4, and 5 mins, respectively (808 nm, 1.0 W/cm<sup>2</sup>). The same procedures were repeated at 15 °C and 8 °C to evaluate the relationship between temperature and dissociation of ICG@HES-SS-DOX NP. The morphologies were characterized by TEM. The count rates and size distribution were recorded by dynamic light scattering (DLS, Nano-ZS90, Malvern). The absorbance of each group was measured by UV/Vis. The temperature was recorded at 30 s intervals using an infrared imaging camera.

### **Penetration of ICG@HES-SS-DOX NP in H22 tumor spheroids**

To prepare the three-dimensional tumor spheroids, H22 cells were seeded in fibrin gel<sup>3</sup>. Briefly, the fibrinogen/cell mixtures were acquired by mixing 2 mg/mL fibrinogen with the same volume of cell solution (1.6×10<sup>4</sup> cells/mL)<sup>4</sup>. 50 µL fibrinogen/cell mixtures were then seeded into each well of 96 well-plates pre-added with 1 µL thrombin (0.1 U/µL). The plate was incubated in cell culture incubator for 15 min and then 0.2 mL RPMI 1640 medium containing 10% FBS was added. Five days after the cells were seeded, tumor spheroids were treated with free DOX, HES-SS-DOX, 7.5 wt% ICG@HES-SS-DOX NP, 7.5 wt% ICG@HES-SS-DOX NP and 5 min NIR stimulating (808 nm, 1.0 W/cm<sup>2</sup>), 12.5 wt%

ICG@HES-SS-DOX NP, 12.5 wt% ICG@HES-SS-DOX NP and 5 min stimulating (808 nm, 1.0 W/cm<sup>2</sup>) at an equivalent concentration of DOX (5 µg/mL). After 4 h of incubation, the spheroids were rinsed with cold PBS buffer for three times and fixed with 4% paraformaldehyde for 15 min. Then the spheroids were transferred to glass bottom petri-dish and covered by glycerophosphate. Fluorescent intensity was recorded by a confocal laser scanning microscopy (CLSM, FV1000, Olympus).

#### **Penetration of ICG@HES-SS-DOX NP in H22 tumor bearing mice**

Male BALB/C mice bearing H22 tumor ( $\approx 200 \text{ mm}^3$ ) were randomly assigned into 6 groups (n=3) and intravenously injected with DOX, HES-SS-DOX, 7.5 wt% ICG@HES-SS-DOX NP, 7.5 wt% ICG@HES-SS-DOX NP, 12.5 wt% ICG@HES-SS-DOX NP and 12.5 wt% ICG@HES-SS-DOX NP (4 mg/kg DOX). After 1 hour, one group of 7.5 wt% ICG@HES-SS-DOX NP and one group of 12.5 wt% ICG@HES-SS-DOX NP were stimulated by NIR for 10 minutes (808 nm, 1.0 W/cm<sup>2</sup>). Then, the mice were sacrificed at 4 h after laser irradiation. The tumors were excised and sectioned into 10 µm thick slices with a cryostat. The slices were briefly fixed with cold acetone, incubated with FITC-CD31 and DAPI. Samples were observed by confocal laser scanning microscopy (CLSM, FV1000, Olympus). Penetration distances were calculated using simulated scatter diagrams<sup>5</sup> based on five confocal images, as shown in Figure S20.

#### **Live Subject Statement**

All animal procedures were performed in accordance with the internationally accepted principles and Guidelines for the Care and Use of Laboratory Animals of Huazhong University of Science and Technology and the experiment protocols were approved by the Institutional Animal Ethical Committee of Huazhong University of Science and Technology. All efforts were made to minimize suffering.

## Supplementary Figures

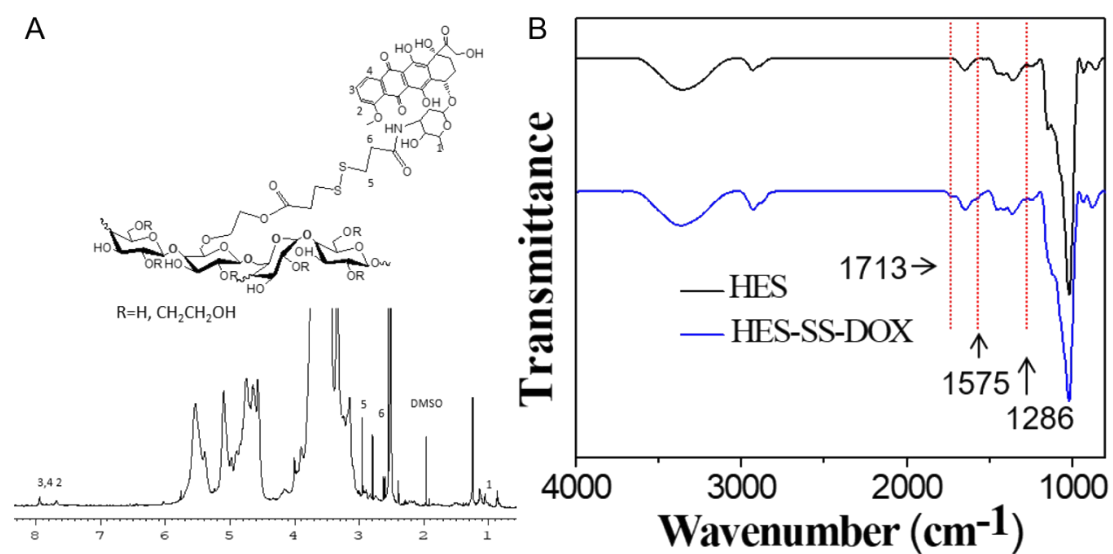


**Figure S1.** Characterization of HES-SS-DOX. (A) <sup>1</sup>H-NMR of HES-SS-DOX; (B) FTIR of HES and HES-SS-DOX.

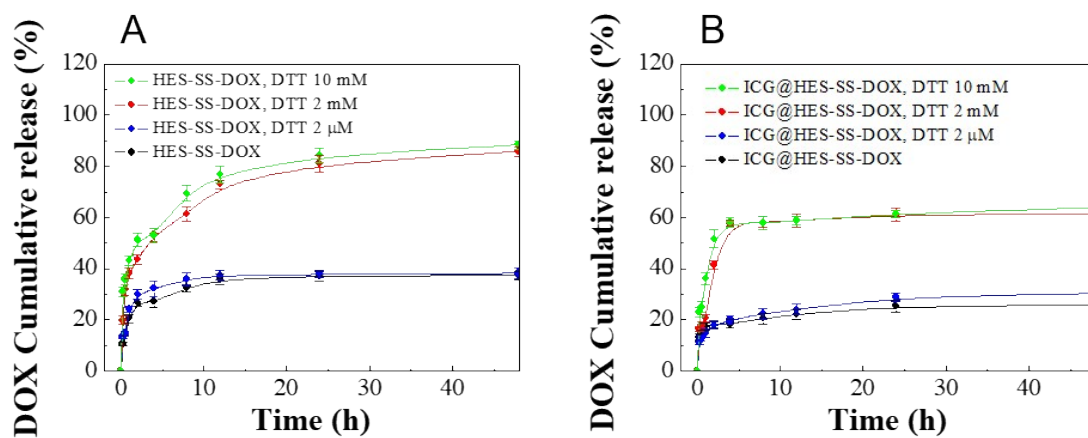


**Figure S2.** Redox responsive property of HES-SS-DOX and ICG@HES-SS-DOX NP. (A) cumulative DOX release from HES-SS-DOX at different concentration of DTT; (B) cumulative DOX release from ICG@HES-SS-DOX NP at different concentration of DTT.

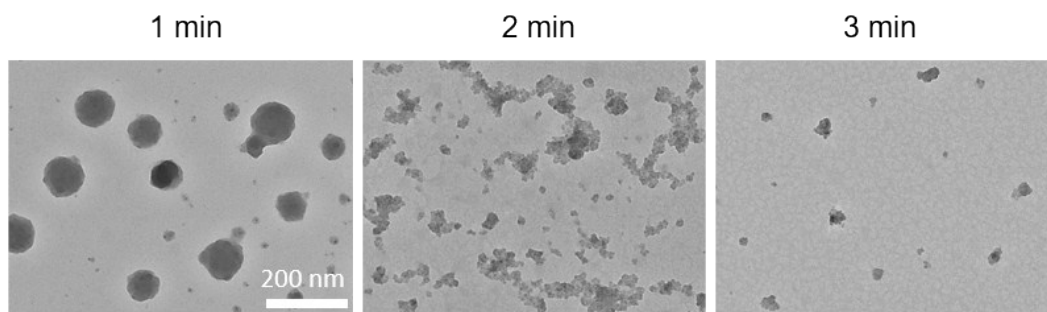


**Figure S3.** Morphology of ICG@HES-SS-DOX NP stimulated by NIR (808 nm, 1.0 W/cm<sup>2</sup>) for 1 min, 2 min and 3 min, respectively, as measured by TEM. The scale bar is 200 nm and applied for all images.

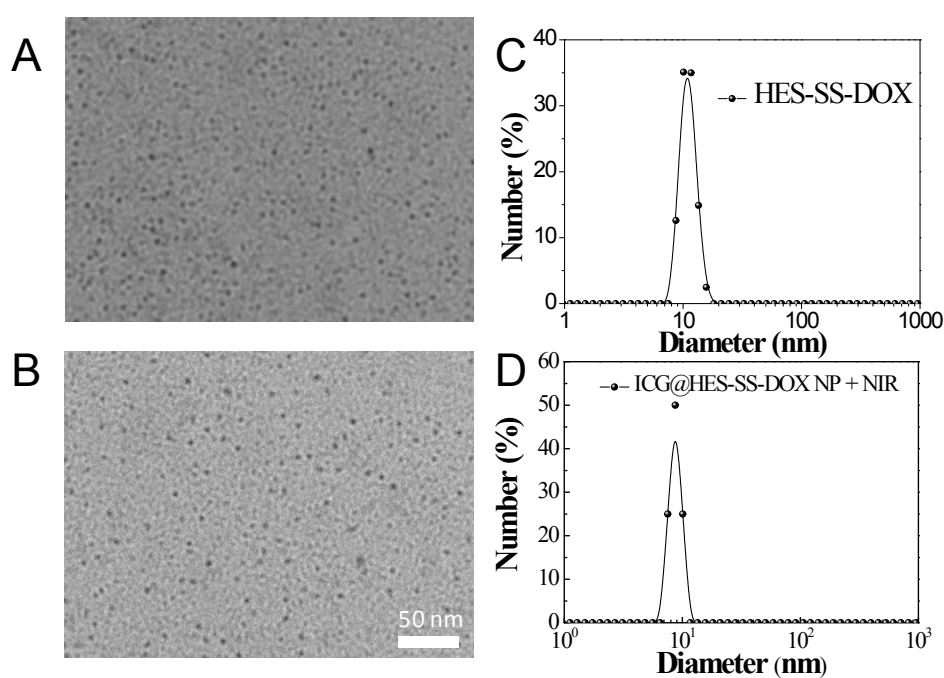


**Figure S4.** Characterization of HES-SS-DOX and ICG@HES-SS-DOX NP stimulated by NIR (808 nm, 1.0 W/cm<sup>2</sup>) for 5 min. Morphology of HES-SS-DOX (A) and ICG@HES-SS-DOX NP stimulated by NIR (B) as measured by TEM; (C) Size distribution of HES-SS-DOX (A) and ICG@HES-SS-DOX NP stimulated by NIR (D) as measured by DLS. The scale bar is 50 nm and applied for images shown in A and B.

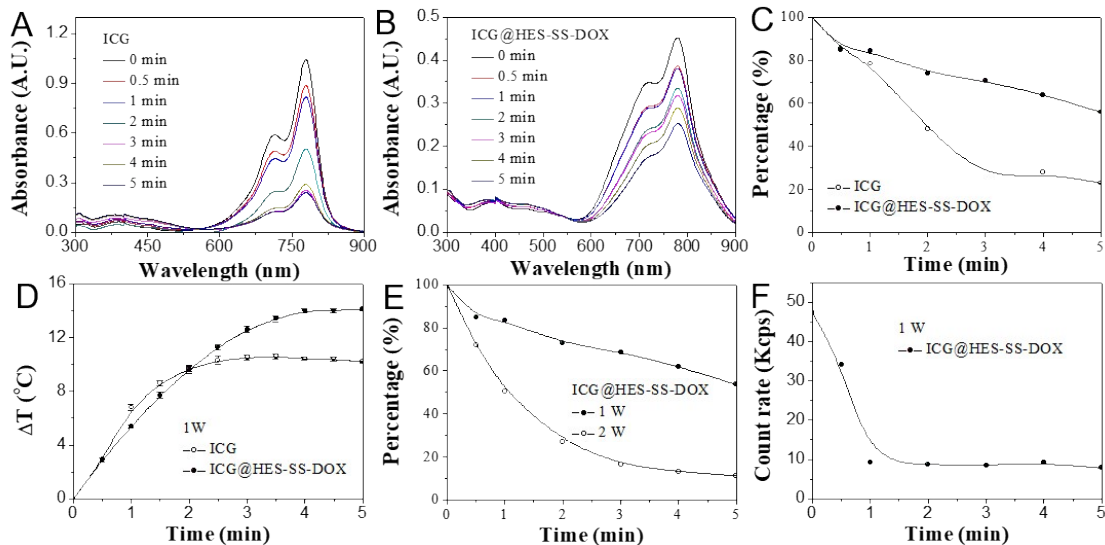


**Figure S5.** Degradation process of ICG (10  $\mu\text{g/mL}$ ) under NIR laser at 25  $^{\circ}\text{C}$  in deionized water. (A) absorbance of ICG under NIR laser (808 nm, 1.0  $\text{W/cm}^2$ ) for different time; (B) absorbance of ICG@HES-SS-DOX NP under NIR laser for different time; (C) absorbance at 780 nm under NIR laser as a function of time; (D) Photothermal response of ICG and ICG@HES-SS-DOX NP under NIR laser (808 nm, 1.0  $\text{W/cm}^2$ ); (E) degradation of ICG@HES-SS-DOX NP at 780 nm under NIR laser (808 nm) of varied power (1.0  $\text{W/cm}^2$  and 2.0  $\text{W/cm}^2$ ); (F) Count rate of ICG@HES-SS-DOX NP under NIR laser (808 nm, 1.0  $\text{W/cm}^2$ ) as a function of time.

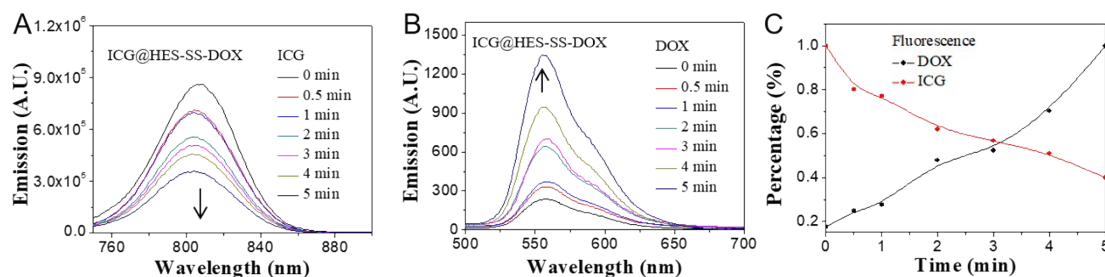


**Figure S6.** Degradation of ICG is accompanied with DOX fluorescence recovery as ICG@HES-SS-DOX dissociates. (A) ICG fluorescence as a function of NIR stimulating time; (B) DOX fluorescence as a function of NIR stimulating time; (C) Recovery of DOX emission at 556 nm is accompanied with the decreasing of ICG emission at 805 nm as a function of NIR stimulating time.

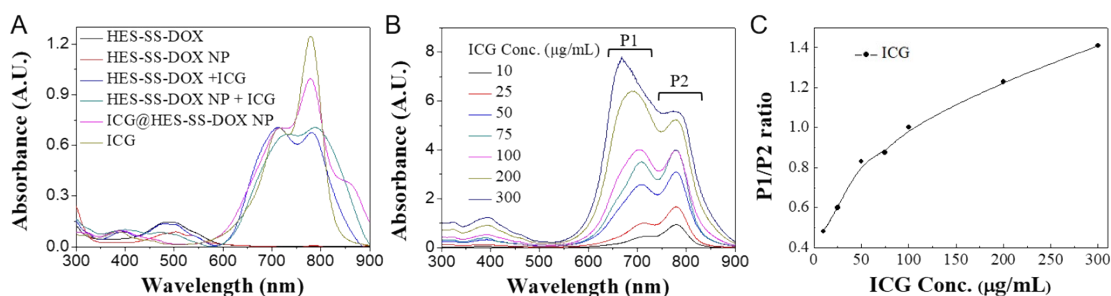


**Figure S7.** Assembling of ICG in deionized water dictated ICG absorbance peak at 700 nm and 780 nm. (A) absorbance of various formulations in the range of 300 and 900 nm; (B) UV absorbance of ICG at different concentration; (C) ratio of Peak 1 (700 nm) and Peak 2 (780 nm) at different ICG concentration.

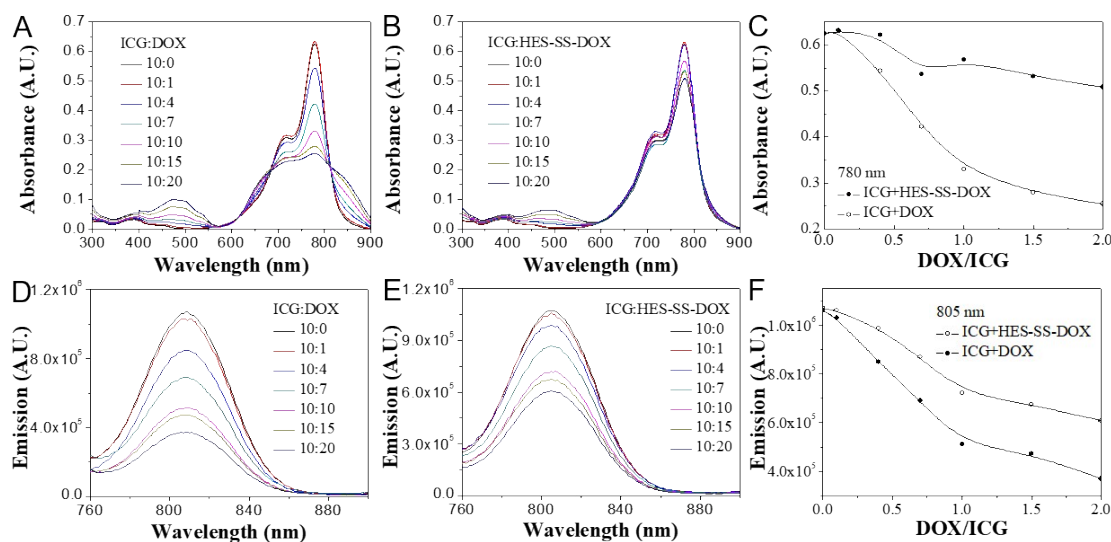


**Figure S8.** Interaction between ICG and HES-SS-DOX. (A) absorbance of ICG and DOX mixture with varied ratio of ICG: DOX (w/w); (B) absorbance of ICG and HES-SS-DOX with varied ratio of ICG: HES-SS-DOX (w/w); (C) absorbance at 780 nm obtained from A and B; (D) Fluorescence of ICG and DOX mixture with varied ratio of ICG:DOX; (E) Fluorescence of ICG and HES-SS-DOX with varied ratio of ICG:HES-SS-DOX; (F) emission at 805 nm obtained from D and E.

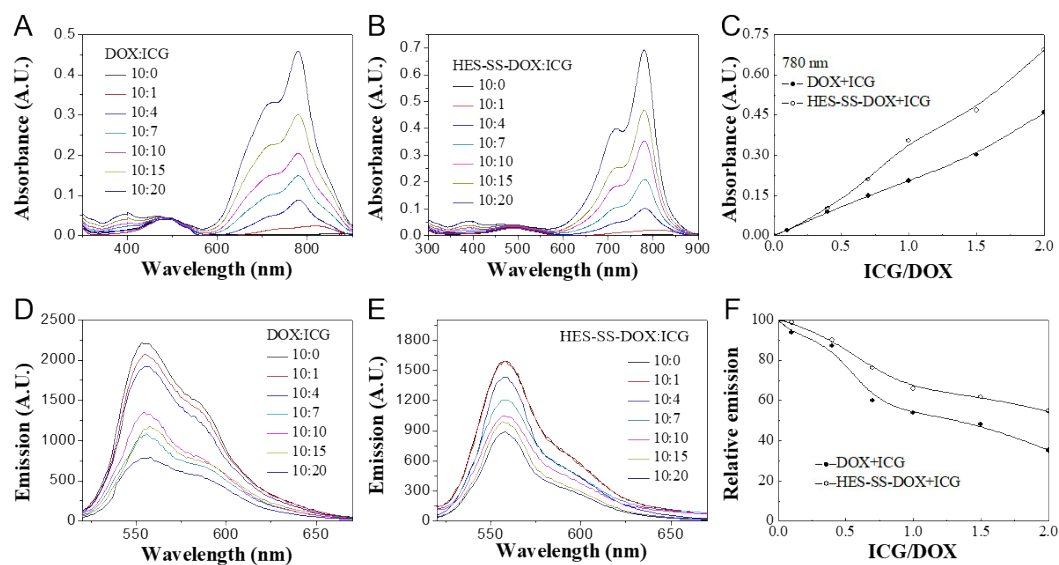


**Figure S9.** Interaction between HES-SS-DOX and ICG. (A) absorbance of ICG and DOX mixture with varied ratio of ICG:DOX (w/w); (B) absorbance of ICG and HES-SS-DOX with varied ratio of ICG:HES-SS-DOX (w/w); (C) absorbance at 780 nm obtained from A and B; (D) Fluorescence of ICG and DOX mixture with varied ratio of ICG:DOX; (E) Fluorescence of ICG and HES-SS-DOX with varied ratio of ICG:HES-SS-DOX; (F) relative emission at 560 nm obtained from D and E.

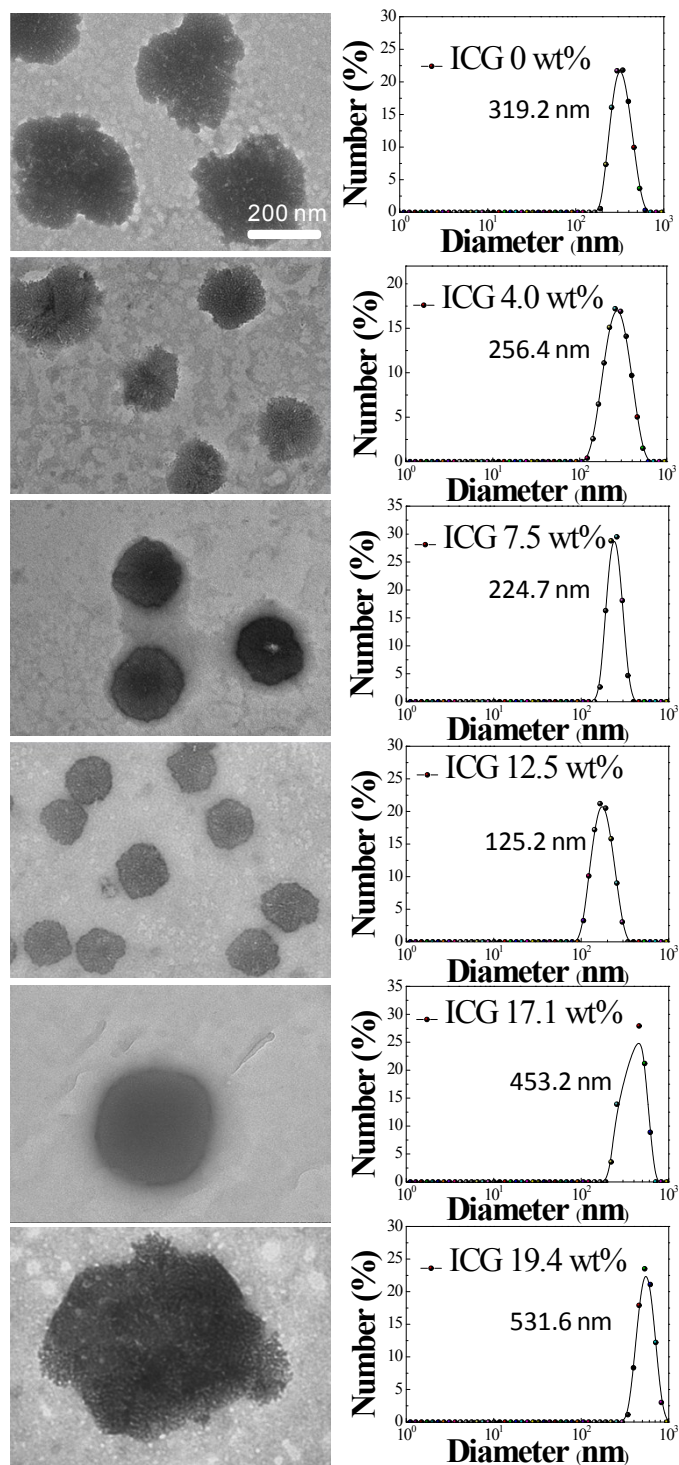


**Figure S10.** Morphology and size distribution of ICG@HES-SS-DOX NPs of different ICG loading content as measured by TEM and DLS. The scale bar is 200 nm and applied for all TEM images.

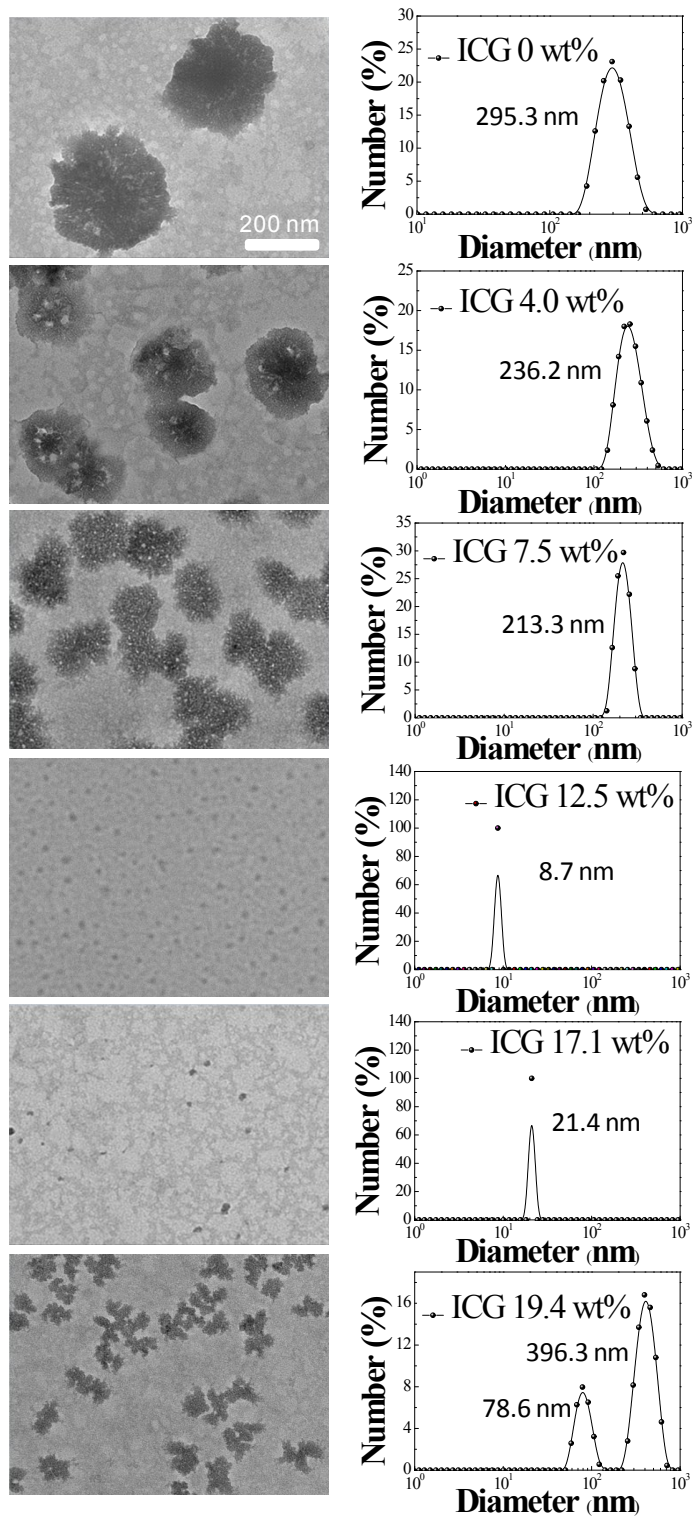


**Figure S11.** Morphology and size distribution of ICG@HES-SS-DOX NPs of different ICG loading content after exposed to NIR light for 5 mins, as measured by TEM and DLS. The scale bar is 200 nm and applied for all TEM images.

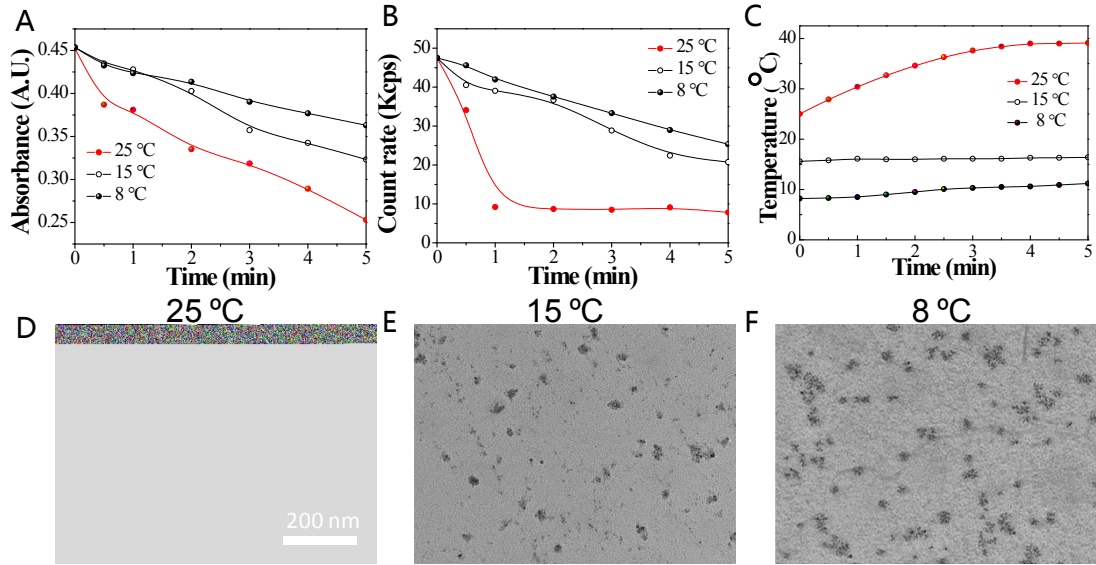


**Figure S12.** The effect of temperature on the dissociation of ICG@HES-SS-DOX NP. (A) UV absorbance of ICG@HES-SS-DOX at 780 nm at 25 °C, 15 °C and 8 °C after NIR stimulating for different time; (B) count rates of ICG@HES-SS-DOX at 25 °C, 15 °C and 8 °C after NIR stimulating for different time; (C) Temperature of ICG@HES-SS-DOX at 25 °C, 15 °C and 8 °C after NIR stimulating. Morphologies of ICG@HES-SS-DOX NP after exposed to NIR stimulating for 5 min at 25 °C (D), 15 °C (E), and 8 °C (F), respectively. The scale bar is 200 nm for images (D-F).

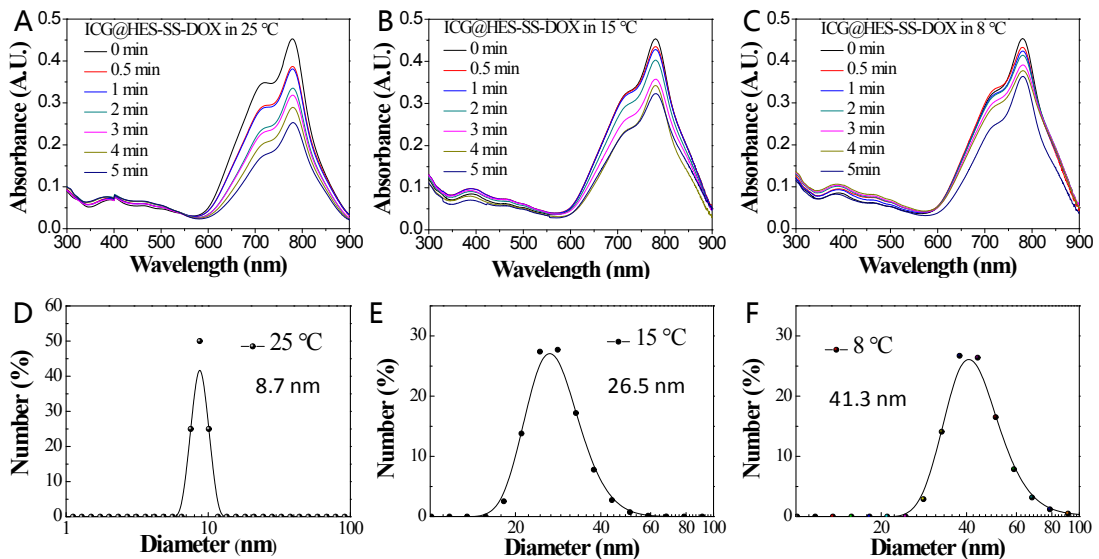


**Figure S13.** The effect of temperature on the dissociation of ICG@HES-SS-DOX NP. (A) UV absorbance of ICG@HES-SS-DOX at 25 °C stimulated by NIR for different time; (B)

UV absorbance of ICG@HES-SS-DOX at 15 °C stimulated by NIR for different time; (C) UV absorbance of ICG@HES-SS-DOX at 8 °C stimulated by NIR for different time; Size distribution of ICG@HES-SS-DOX NP stimulated by NIR for 5 min at 25 °C (D), 15 °C (E), and 8 °C (F), respectively, in deionized water.

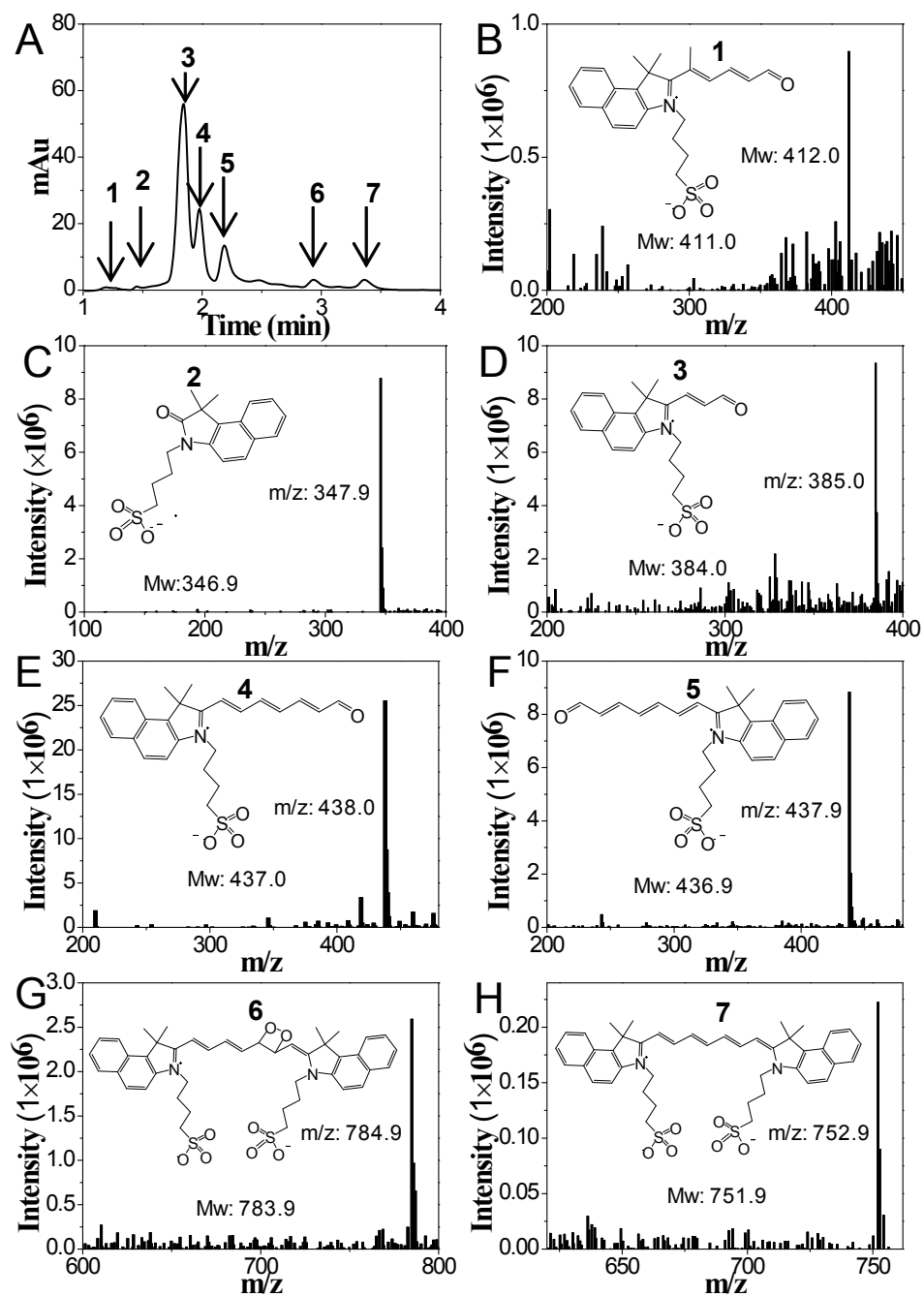


**Figure S14.** Degradation products of ICG in de-ionized water in 7 days as measured by HPLC-MS. (A) HPLC result of compound 1–7 (detected by UV absorbance at 290 nm). (B–

H) MS of spectra of the compound 1-7.

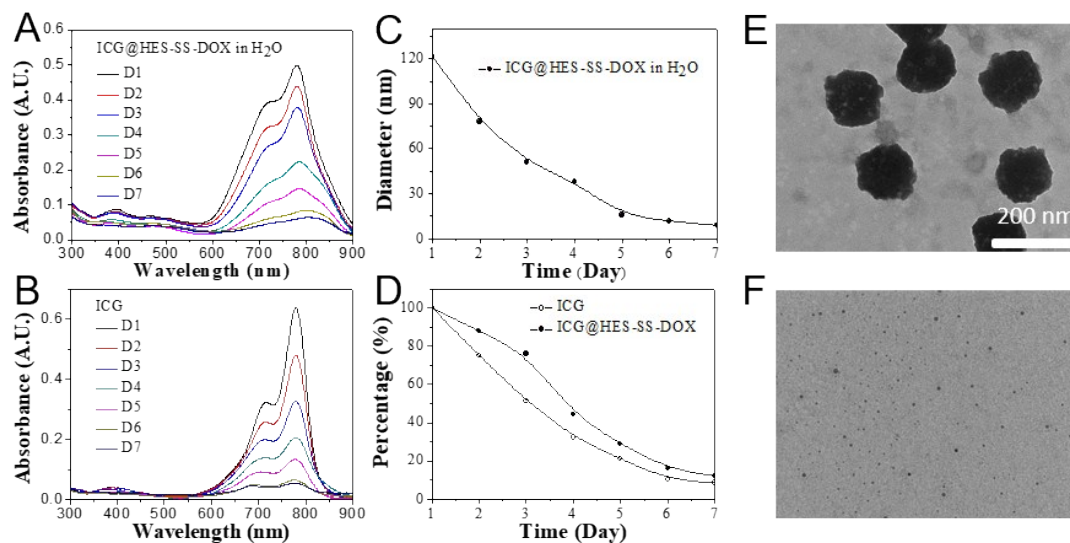


**Figure S15.** Dissociation of ICG@HES-SS-DOX NP in de-ionized water as a function of time. (A) UV absorbance of ICG@HES-SS-DOX NP at different time; (B) UV absorbance of ICG at different time; (C) Average diameter of ICG@HES-SS-DOX NP at different time; (D) percentage of ICG in free ICG and ICG@HES-SS-DOX NP obtained from A and B; Morphology of ICG@HES-SS-DOX NP at day 1 (E) and day 7 (F) as measured by TEM. The scale bar is 200 nm and applied for both E and F.

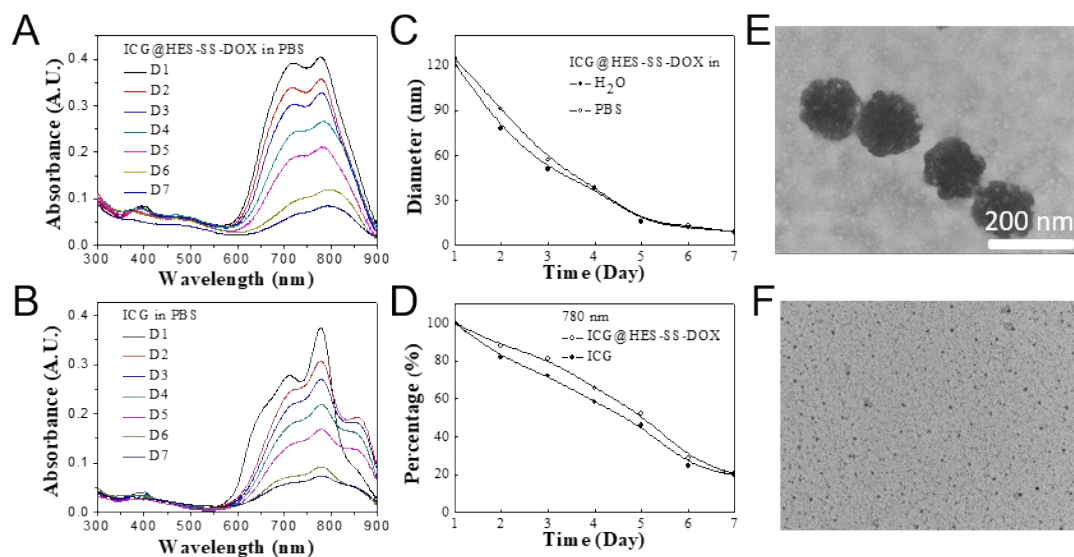


**Figure S16.** Dissociation of ICG@HES-SS-DOX NP in PBS buffer as a function of time. (A) UV absorbance of ICG@HES-SS-DOX NP at different time; (B) UV absorbance of ICG

at different time; (C) Average diameter of ICG@HES-SS-DOX NP in de-ionized water and PBS buffer as a function of time; (D) percentage of ICG in free ICG and ICG@HES-SS-DOX NP obtained from A and B; Morphology of ICG@HES-SS-DOX NP at day 1 (E) and day 7 (F) as measured by TEM. The scale bar is 200 nm and applied for both E and F.

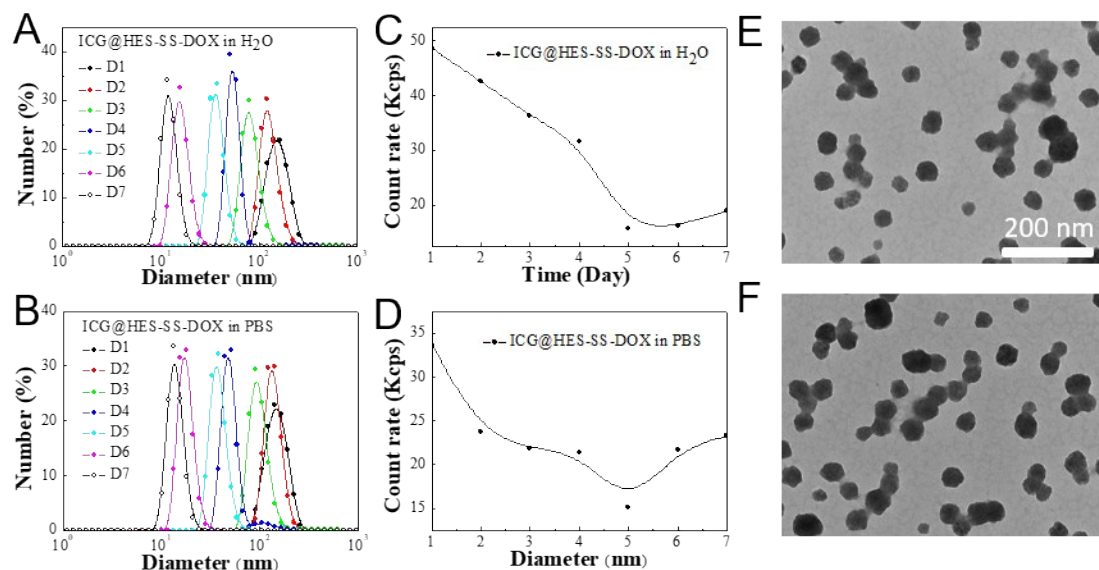


**Figure S17.** Dissociation of ICG@HES-SS-DOX NP in de-ionized water and PBS buffer. (A) Diameter distribution of ICG@HES-SS-DOX NP in de-ionized water during 7 days; (B) Diameter distribution of ICG@HES-SS-DOX NP in PBS buffer during 7 days; (C) Count rate of ICG@HES-SS-DOX NP in deionized water in 7 days; (D) Count rate of ICG@HES-SS-DOX NP in PBS buffer in 7 days; morphology of ICG@HES-SS-DOX NP at day 4 in de-ionized water (E) and PBS buffer (F) as measured by TEM. The scale bar is 200 nm and applied for both E and F.

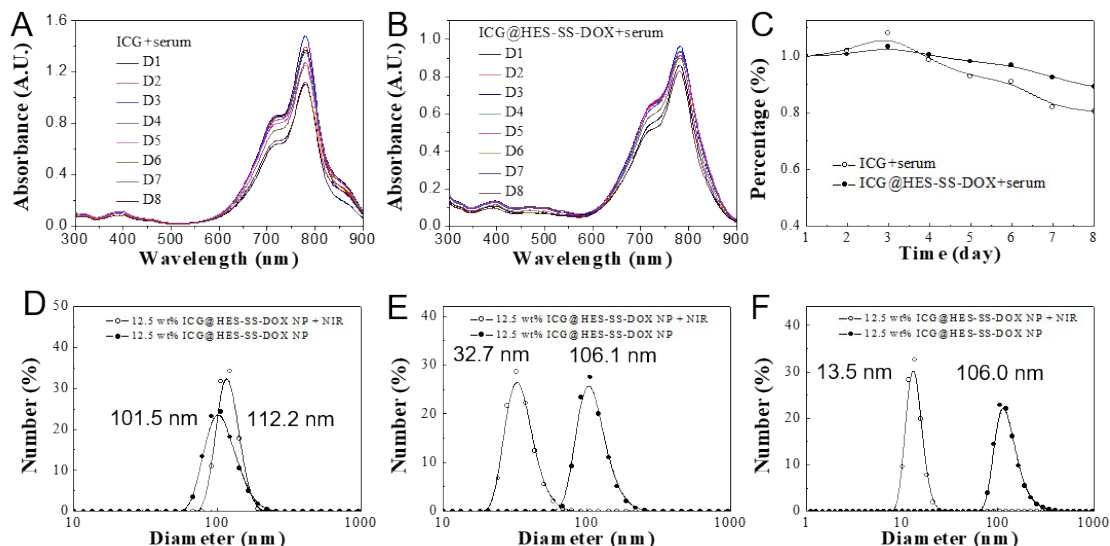


**Figure S18.** Stability of ICG@HES-SS-DOX (12.5wt %) NP in mice serum. (A) UV absorbance of free ICG incubated with serum in 8 days; (B) UV absorbance of ICG@HES-SS-DOX NP incubated with serum in 8 days; (C) Percentage of ICG from free ICG and ICG@HES-SS-DOX NP obtained from A and B; Size distribution of ICG@HES-SS-DOX NP before and after 5 mins NIR (808 nm, 1.0 W/cm<sup>2</sup>) stimulation at day 3 (D), day 4 (E), and day 8 (F), respectively.

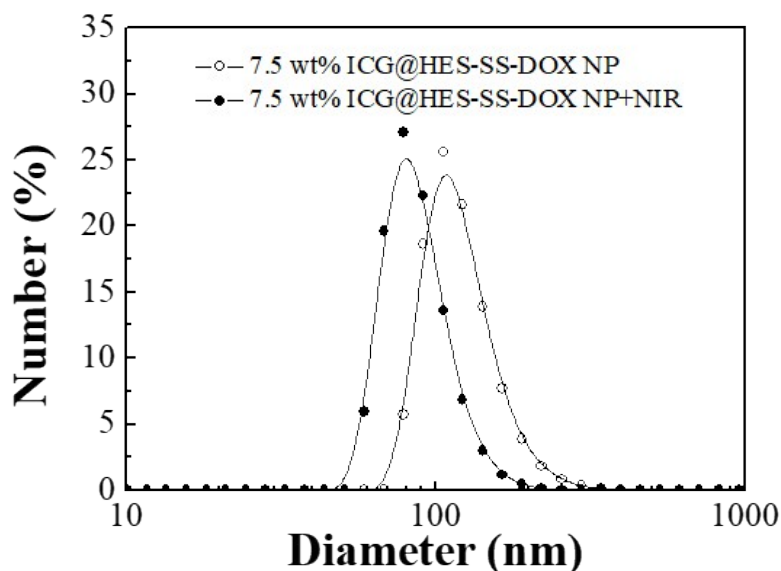


**Figure S19.** Size distribution of ICG@HES-SS-DOX (7.5wt %) NP in mice serum before and after 5 mins NIR (808 nm, 1.0 W/cm<sup>2</sup>) stimulation at day 8.

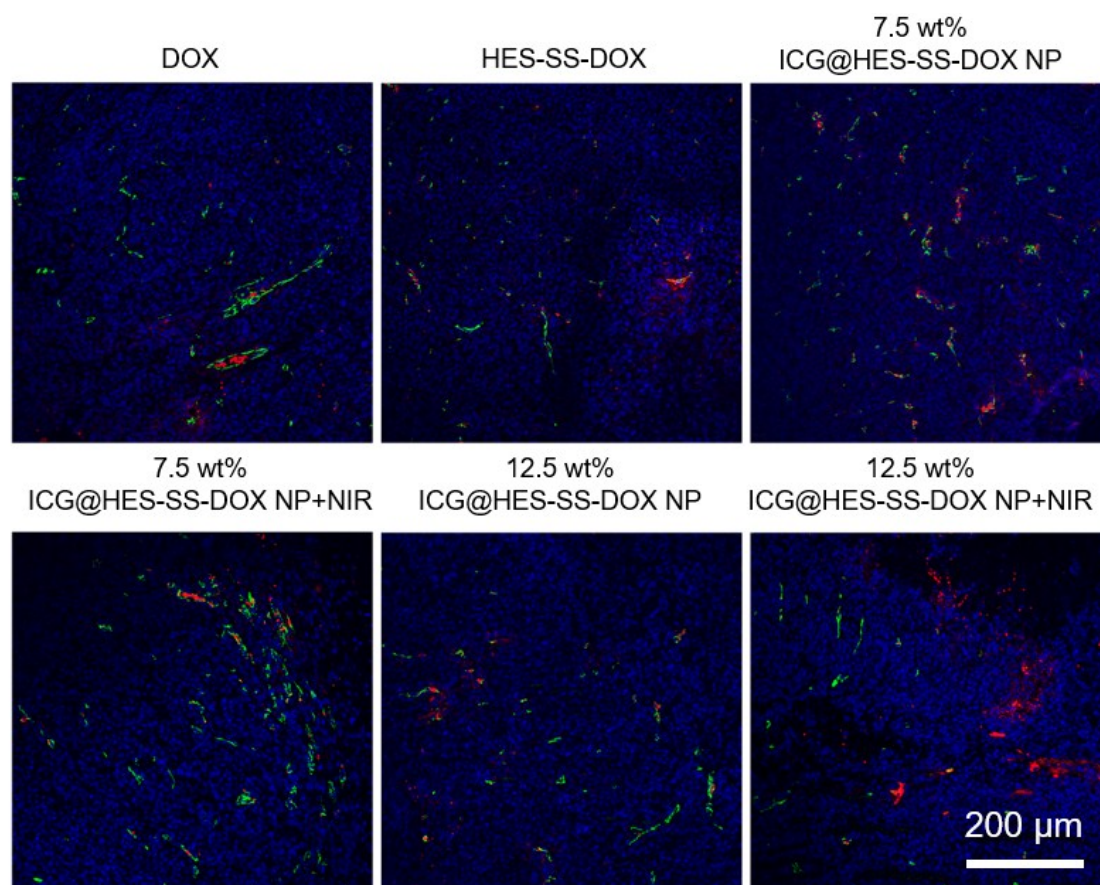


**Figure S20.** Ex vivo CLSM images of tumor sections 1 h post injection (equivalent to 4.0 mg DOX and 7.5 mg ICG /kg bodyweight for 7.5wt% ICG@HES-SS-DOX NP and 4.0 mg DOX and 12.5 mg ICG /kg bodyweight for 12.5wt% ICG@HES-SS-DOX NP). Tumor blood vessels were stained with green CD31 marker, tumor nucleus was stained with DAPI, and DOX showed red fluorescence. The scale bar is 200  $\mu\text{m}$  and applied for all images.

## References

1. H. Hu, Y. Li, Q. Zhou, Y. Ao, C. Yu, Y. Wan, H. Xu, Z. Li and X. Yang, *ACS Applied Materials & Interfaces*, 2016, **8**, 30833-30844.
2. H. Hu, C. Xiao, H. Wu, Y. Li, Q. Zhou, Y. Tang, C. Yu, X. Yang and Z. Li, *ACS Applied Materials & Interfaces*, 2017, **9**, 42225-42238.
3. J. Liu, Y. Tan, H. Zhang, Y. Zhang, P. Xu, J. Chen, Y.-C. Poh, K. Tang, N. Wang and B. Huang, *Nature Materials*, 2012, **11**, 734-741.
4. H. Yang, Q. Wang, Z. Li, F. Li, D. Wu, M. Fan, A. Zheng, B. Huang, L. Gan, Y. Zhao and X. Yang, *Nano Letters*, 2018, **18**, 7909-7918.
5. T. Wei, J. Liu, H. Ma, Q. Cheng, Y. Huang, J. Zhao, S. Huo, X. Xue, Z. Liang and X.-J. Liang, *Nano Letters*, 2013, **13**, 2528-2534.